

Complexation of Phosphoric Acid Diesters with Polyaza-Clefts in Chloroform: Effects of Phosphodiester Dimerization, Changing Cavity Size, and Preorganizing Amine Recognition Units

Feiya Chu, Lisa S. Flatt, and Eric V. Anslyn*

Contribution from the Department of Chemistry and Biochemistry,
The University of Texas at Austin, Austin, Texas 78712

Received November 11, 1993*

Abstract: Polyaza-receptors 1–3 and pyridine were investigated as complexing agents for phosphoric acid diesters in chloroform. These receptors were used to determine the optimum cavity size for complexing phosphoric acid diesters and to measure the strength of interactions formed by individual host hydrogen bond donors and acceptors. Inflections in either the ^{31}P or ^1H NMR isotherms were found for all receptors. The NMR data indicate equilibria involving host–guest and host–(guest) $_2$ complexes. Formation of 2:1 guest-to-host complexes is a result of the large dimerization constants for phosphoric acid diesters. The association constant of dinaphthyl hydrogen phosphate to dibenzyl hydrogen phosphate was determined to be $6.5 \times 10^4 \text{ M}^{-1}$. Since strong aggregation of the phosphoric acid diesters complicated the analysis of the NMR data, the binding constants with the polyaza-receptors were determined by a combination of fluorescence and UV/vis techniques. The 1:1 binding constants measured in chloroform for dibenzyl hydrogen phosphate or dinaphthyl hydrogen phosphate with receptors 1–3 and pyridine are 7.8×10^3 , 8.9×10^4 , 1.3×10^3 , and $3.6 \times 10^2 \text{ M}^{-1}$, respectively. The strength of complexation of phosphoric acid diesters to the polyaza-clefts is dependent upon the number of hydrogen bonds formed and the receptor cavity size. The major driving force for complexation arises from the hydrogen bond formed between the phosphoric acid hydrogen and the pyridine nitrogen of a receptor.

Introduction

Phosphodiesterases play a variety of essential roles in biological processes. They are involved in genetic information storage¹ and energy transduction.² In addition, chemotherapeutic and antiviral drugs have phosphates as integral structural components.³ Therefore, hydrogen-bonding receptors for phosphate esters have received attention due to possible pharmaceutical applications. One area of interest is transport of phosphates through low dielectric media for use as antiviral adjuncts.⁴ Another area is electrophilic activation of polynucleotides toward transesterification or hydrolysis.⁵

There have been a number of published reports detailing strategies for complexing phosphodiesterases and phosphoric acids.^{6–12}

A typical strategy is ion pairing the phosphate moiety with an ammonium or guanidinium^{5a,6} and imparting specificity by incorporating heterocycles for base pairing and/or aromatic rings for π stacking.⁷ Tabushi showed that simple ammonium salts transport nucleotides through chloroform, but methods to impart selectivity were not examined (Figure 1A).⁸ Sessler has elaborated simple ammoniums and expanded porphyrins for the transport of phosphates.⁹ He has recently incorporated a cytosine into an expanded porphyrin and accomplished the selective transport of guanine 5'-monophosphate through chloroform (Figure 1B).¹⁰ Rebek and de Mendoza have used a bicyclic guanidinium to target nucleotide phosphates and have used Watson–Crick and Hoogstine base pairing for imparting selectivity among the four DNA heterocyclic bases (Figure 1C).¹¹

Currently, we are examining polyaza-clefts for the complexation of phosphodiesterases in both low-¹³ and high-dielectric¹⁴ media as a means of achieving transport and electrophilic activation.¹⁵ The design of the receptors features four hydrogen-bonding groups

* Abstract published in *Advance ACS Abstracts*, April 1, 1994.

(1) Saenger, W. *Principles of Nucleic Acid Structure*; Springer-Verlag: New York, 1984.

(2) Devlin, T. M. *Textbook of Biochemistry with Clinical Correlations*; Wiley Medical: New York, 1982.

(3) Revankar, G. R.; Huffman, J. H.; Allen, L. B.; Sidwell, R. W.; Robins, R. K.; Tolman, R. L. *J. Med. Chem.* **1975**, *18*, 721–726. Revankar, G. R.; Huffman, J. H.; Sidwell, R. W.; Tolman, R. L.; Robins, R. K.; Allen, L. B. *J. Med. Chem.* **1976**, *19*, 1026–1028. *Approaches to Antiviral Agents*; Harnden, M. R., Ed.; VCH: Deerfield Beach, FL, 1985.

(4) Christensen, H. N. *Biological Transport*, 2nd ed.; Benjamin Press: New York, 1975; Chapter 10.

(5) (a) For a review of guanidinium-induced activation see: Hannon, C. L.; Anslyn, E. V. The Guanidinium Group: Its Biological Role and Synthetic Analogs. In *Bioorganic Chemistry Frontiers*; Dugas, H., Ed.; Springer Verlag: Berlin, 1993; Vol. 3, p 193. (b) For a review of metal-induced activation see: Chin, J. *Acc. Chem. Res.* **1991**, *24*, 145.

(6) Kodama, M.; Kimura, E.; Yamaguchi, S. *J. Chem. Soc., Dalton Trans.* **1980**, 2536–2538. Kimura, E.; Sakonaka, A.; Yatsunami, T.; Kodama, M. *J. Am. Chem. Soc.* **1981**, *103*, 3041–3045. Dietrich, B.; Hosseini, M. W.; Lehn, J. M.; Sessions, R. B. *J. Am. Chem. Soc.* **1981**, *103*, 1282–1283. Marecek, J. F.; Fischer, P. A.; Burrows, C. J. *Tetrahedron Lett.* **1988**, *29*, 6231–6234. Kimura, E. *Top. Curr. Chem.* **1985**, *128*, 113–141. Mertes, M. P.; Mertes, K. B. *Acc. Chem. Res.* **1990**, *23*, 413–418. Hosseini, M. W.; Blacker, A. J.; Lehn, J.-M. *J. Am. Chem. Soc.* **1990**, *112*, 3896–3904. Kimura, E.; Kuramoto, Y.; Koike, T.; Fujioka, H.; Kodama, M. *J. Org. Chem.* **1990**, *55*, 42–46. Aoyama, Y.; Nonaka, S.-I.; Motomura, T.; Toi, H.; Ogoshi, H. *Chem. Lett.* **1991**, 1241–1244. Claude, S.; Lehn, J.-M.; Schmidt, F.; Vigneron, J.-P. *J. Chem. Soc., Chem Commun.* **1991**, 1182–1185.

(7) For receptors using base pairing and π stacking see: Conn, M. M.; Deslongchamps, G.; de Mendoza, J.; Rebek, J., Jr. *J. Am. Chem. Soc.* **1993**, *115*, 3548 and references therein.

(8) Tabushi, I.; Kobuke, Y.; Imuta, J.-I. *J. Am. Chem. Soc.* **1981**, *103*, 6152–6157.

(9) Furuta, H.; Cyr, M. J.; Sessler, J. L. *J. Am. Chem. Soc.* **1991**, *113*, 6677–6678. Furuta, H.; Furuta, K.; Sessler, J. L. *J. Am. Chem. Soc.* **1991**, *113*, 4706–4707. Furuta, H.; Magda, D.; Sessler, J. L. *J. Am. Chem. Soc.* **1991**, *113*, 978–985.

(10) Král, V.; Sessler, J. L.; Furuta, H. *J. Am. Chem. Soc.* **1992**, *114*, 8704–8705.

(11) Deslongchamps, G.; Galan, A.; deMendoza, J.; Rebek, J., Jr., *Angew. Chem., Int. Ed. Engl.* **1992**, *31*, 61–63.

(12) Rudkevich, D. M.; Stauthamer, W. P. R.; Verboom, W.; Engbersen, J. F. J.; Harkema, S.; Reinhoudt, D. N. *J. Am. Chem. Soc.* **1992**, *114*, 9671–9673.

(13) Flatt, L. S.; Lynch, V.; Anslyn, E. V. *Tetrahedron Lett.* **1992**, *33*, 2785–2788.

(14) (a) Ariga, K.; Anslyn, E. V. *J. Org. Chem.* **1992**, *57*, 417–419. (b) Kneeland, D. M.; Ariga, K.; Lynch, V. M.; Huang, C.-Y.; Anslyn, E. V. *J. Am. Chem. Soc.* **1993**, *115*, 10042–10055.

(15) Smith, J.; Ariga, K.; Anslyn, E. V. *J. Am. Chem. Soc.* **1993**, *115*, 362–364.

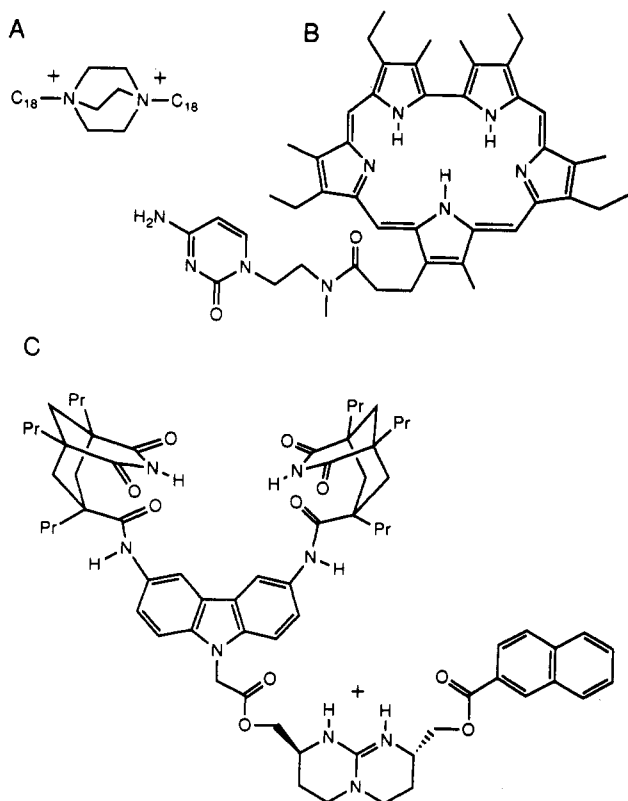


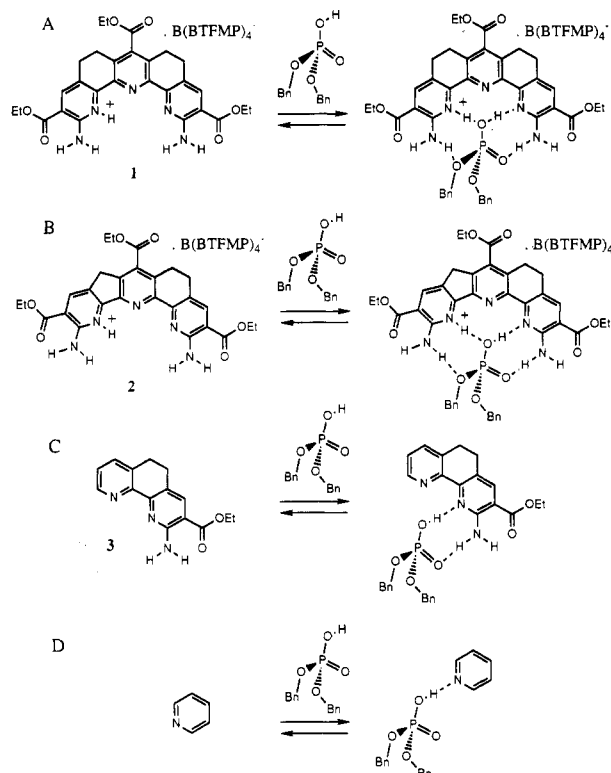
Figure 1. Synthetic phosphate transport and binding systems.

preorganized into a cleft, encapsulating a phosphoric acid diester and shielding it from the surrounding solvent. To increase transport efficiency, we focused our initial efforts on maximizing the free energy of complexation of a phosphoric acid diester. In accomplishing this goal, we encountered three questions. First, is the complexation of phosphoric acid diesters complicated by self-aggregation effects in a low-dielectric solvent? Second, what is the optimum arrangement of four hydrogen bonds for strong phosphodiester complexation? Finally, what is the contribution to free energy of complexation from each hydrogen bond donor and acceptor? This manuscript focuses on complexation of phosphoric acid diesters with polyaza-clefts and describes studies aimed at answering these questions.

Results and Discussion

A. Design Criteria. Receptors 1–3 and pyridine, as well as possible host–guest structures with dibenzyl hydrogen phosphate are shown in Scheme 1. Receptors 1 and 2 possess three hydrogen bond donors and a hydrogen bond acceptor in a spatial array complementary to the acid hydrogen and three oxygens of a tetrahedral phosphoric acid diester.¹⁶ The acceptor is formed from a pyridine, two of the donors are aromatic amines, and one of the donors is a pyridinium. The counterion to the pyridinium

Scheme 1. Host–Guest Complexes [B(BTFMP)₄][−] = tetrakis(3,5-bis(trifluoromethyl)phenyl)borate]



is tetrakis(3,5-bis(trifluoromethyl)phenyl)borate.¹⁷ A critical structural element of these polyaza-clefts is the ethanediyl or methylene linkers that rigidify the pyridines of the terpyridine group into a preorganized cavity.¹⁸ Varying these linkers allows for the cavity size and the twist angle between the peripheral pyridines to be controlled.

It is well precedented that anionic guests such as phosphates and carboxylates associate strongly with cationic hosts in low-dielectric media, such as chloroform, through ion pairing.^{5a,6} However, in determining the optimal spatial positioning of hydrogen bond donors and acceptors for a phosphodiester, we concentrated on binding neutral phosphoric acid benzyl, phenyl, or naphthyl diesters. We avoided maximizing the free energy of complexation by using anionic phosphates, because the resulting very large association in chloroform could possibly mask subtle differences in complementarity.

B. Synthesis. The syntheses of receptors 1 and 3 have been reported in preliminary form,¹⁹ and the details of their syntheses are reported elsewhere.²⁰ To form the unsymmetrical receptor 2, we constructed the central pyridine from two fragments differing in the number of methylenes linking the central and peripheral pyridines. Such a method has been discussed by Thummel,²¹ and ourselves.²⁰ The complete synthetic route for 2 is shown in Scheme 2. Although compound 2 has not been previously reported, we have discussed the details of a very similar synthesis.²⁰ Therefore, only the preparation of the various protonated forms of 2 will be discussed herein.

Free base 2 was purified by crystallization with picric acid. The metathesis to a tetrakis(3,5-bis(trifluoromethyl)phenyl)borate anion¹⁷ was performed in chloroform by stirring the

(16) For other polyaza-receptors see: Kelly, T. R.; Zhao, C.; Bridger, G. J. *J. Am. Chem. Soc.* **1989**, *111*, 3744–3745. Kelly, T. R.; Maguire, M. P. *J. Am. Chem. Soc.* **1987**, *109*, 6549–6551. Pant, N.; Muehldorf, A.; Hamilton, A. D. *Pure Appl. Chem.* **1988**, *60*, 533–538. Jubian, V.; Dixon, R. P.; Hamilton, A. D. *J. Am. Chem. Soc.* **1992**, *114*, 1120–1121. Hamilton, A. D.; Dixon, R. P.; Geib, S. J. *J. Am. Chem. Soc.* **1992**, *114*, 365–366. Vincent, C.; Hirst, S. C.; Garcia-Tellado, F.; Hamilton, A. D. *J. Am. Chem. Soc.* **1991**, *113*, 5466–5467. Zimmerman, S. C.; Zeng, Z.; Wu, W.; Reichert, D. E. *J. Am. Chem. Soc.* **1991**, *113*, 183–196. Bell, T. W.; Liu, J. J. *J. Am. Chem. Soc.* **1988**, *110*, 3673–3674. Hamilton, A. D.; Tecilla, P.; Chang, S.-K. *J. Am. Chem. Soc.* **1990**, *112*, 9586–9590. Caluwe, P.; Majewicz, T. G. *J. Org. Chem.* **1975**, *40*, 2566–2567. Kelly, T. R.; Meghani, P.; Ekkundi, V. S. *Tetrahedron Lett.* **1990**, *31*, 3381–3384. Kelly, T. R.; Bilodeau, M. T.; Bridger, G. J.; Zhao, C. *Tetrahedron Lett.* **1989**, *30*, 2485–2488. Bell, T. W.; Liu, J. *Angew. Chem., Int. Ed. Engl.*, **1990**, *29*, 923–925. Hegde, V.; Madhukar, P.; Madura, J.; Thummel, R. P. *J. Am. Chem. Soc.* **1990**, *112*, 4549–4550. Bell, T. W.; Santora, V. J. *J. Am. Chem. Soc.* **1992**, *114*, 8300–8302.

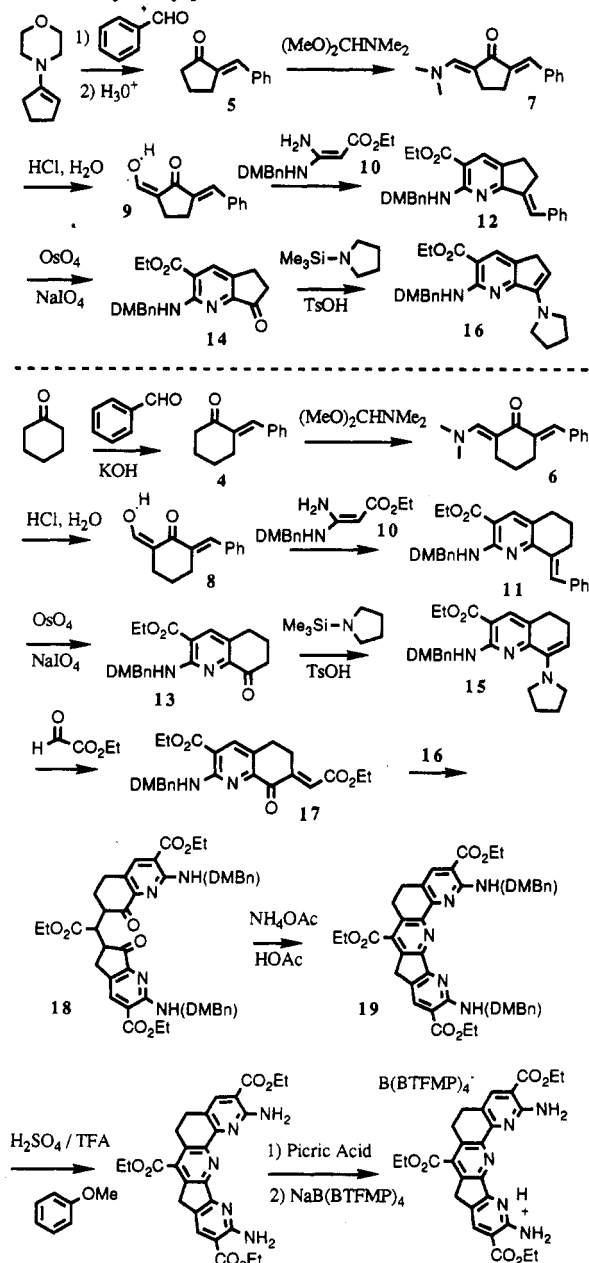
(17) Nishida, H.; Takada, N.; Yoshimura, M.; Sonoda, T.; Kobayashi, H. *Bull. Chem. Soc. Jpn.* **1984**, *57*, 2600–2604.

(18) Such preorganization has been found to be crucial in a similar system. Zimmerman, S. C.; Mrksich, M.; Baloga, M. *J. Am. Chem. Soc.* **1989**, *111*, 8528–8530.

(19) Huang, C.-Y.; Cabell, L. A.; Anslyn, E. V. *Tetrahedron Lett.* **1990**, *31*, 7411–7414.

(20) Huang, C.-Y.; Cabell, L. A.; Anslyn, E. V. *J. Am. Chem. Soc.* **1994**, *116*, 2778–2793.

(21) Thummel, R. P.; Jahng, Y. *J. Org. Chem.* **1985**, *50*, 2407–2412.

Scheme 2. Synthetic Route to **2** [B(BTFMP)₄⁻ = tetrakis(3,5-bis(trifluoromethyl)phenyl)borate; DMBn = 3,4-dimethoxybenzyl]

monopicate salt of **2** with sodium tetrakis(3,5-bis(trifluoromethyl)phenyl)borate salt for several hours, followed by filtration to remove the precipitated sodium picrate.

C. Complexation Studies. i. Host Aggregation. In order for valid conclusions about complementarity differences and free energy changes to be drawn, host oligomerization must be minimized.²² Dilution studies were used to determine concentrations at which the hosts were not aggregated. For example, the ¹H NMR chemical shifts of the peripheral pyridine para protons in **1** were followed upon dilution (Figure 2A) in CDCl₃. The resulting isotherm was modeled with an algorithm for dimerization,²³ giving a dimerization constant (*K*_d) of 375 M⁻¹. On the basis of this *K*_d, the maximum concentration of **1** appropriate for

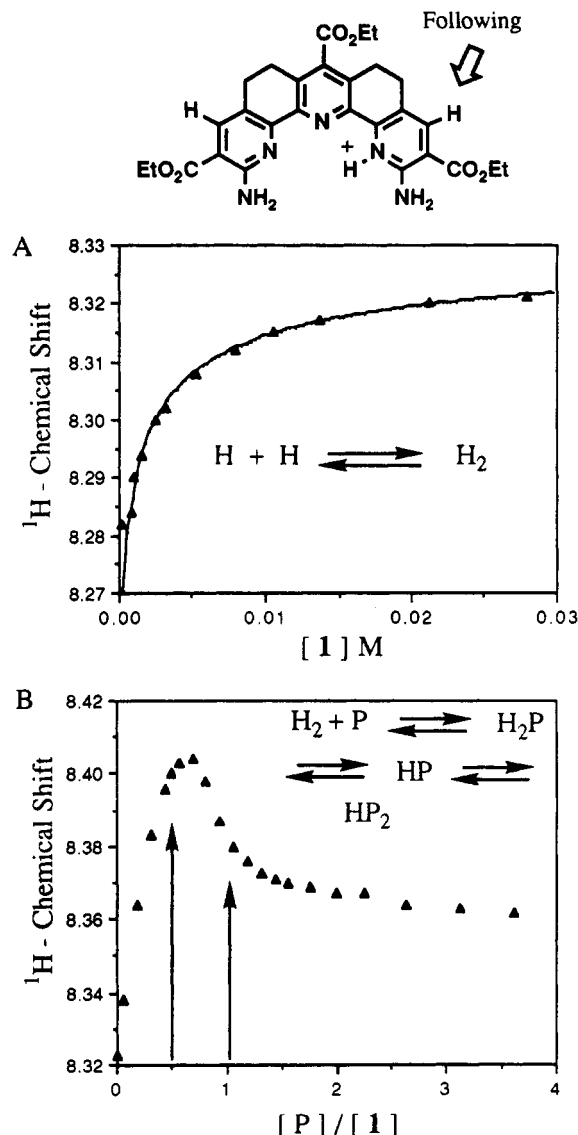


Figure 2. P = dibenzyl hydrogen phosphate, H = **1**. (A) Experimental points for dilution of **1** following the para pyridine ¹H NMR resonance. The line drawn represents the theoretical model for formation of a dimer. (B) Experimental points following the para pyridine ¹H NMR resonance of **1** with incremental increases in the concentration of dibenzyl hydrogen phosphate. Concentration of **1** was 6.45 × 10⁻³ M.

a ¹H NMR titration study should be 3.3 × 10⁻⁴ M. At this concentration, less than 10% of the host should be dimerized. Similar restrictions on the concentration of **2** were employed in the binding studies. At concentrations significantly above this level, host oligomerization should be detected in the NMR isotherms. In confirmation, ¹H NMR titrations performed with **1** (H) showed an inflection near 0.5 equiv of dibenzyl hydrogen phosphate (P), indicative of a H₂P structure (Figure 2B). NMR isotherms performed below 3.3 × 10⁻⁴ M, however, showed no such inflection. The oligomerization of **1** and **2** likely occurs by a pyridine hydrogen bonding to a pyridinium of a second host. In contrast, no significant change in the chemical shifts of pyridine or **3** were observed upon dilution. Thus, as expected, pyridine and **3** are not significantly oligomerized in chloroform.

ii. Complication of NMR Binding Isotherms by Phosphoric Acid Dimerization. Pyridines and arylamines are common building blocks for hydrogen-bonding molecular receptors.¹⁶ As a starting point for deciphering the energetic advantage of preorganizing such groups into a polyaza-cleft, we studied the binding of dibenzyl hydrogen phosphate with the simple aromatic amine pyridine. The goal was to contrast the binding

(22) Salts have a tendency to aggregate in low-dielectric media. Batson, F. M.; Kraus, C. A. *J. Am. Chem. Soc.* **1934**, *56*, 2017–2020. Copenhafer, D. T.; Kraus, C. A. *J. Am. Chem. Soc.* **1951**, *73*, 4557–4561. Bruckenstein, S.; Vanderborgh, N. E. *Anal. Chem.* **1966**, *38*, 687–692.

(23) Connors, K. A. *Binding Constants: The Measurement of Molecular Complex Stability*; Wiley-Interscience: New York, 1987; p 24–28.

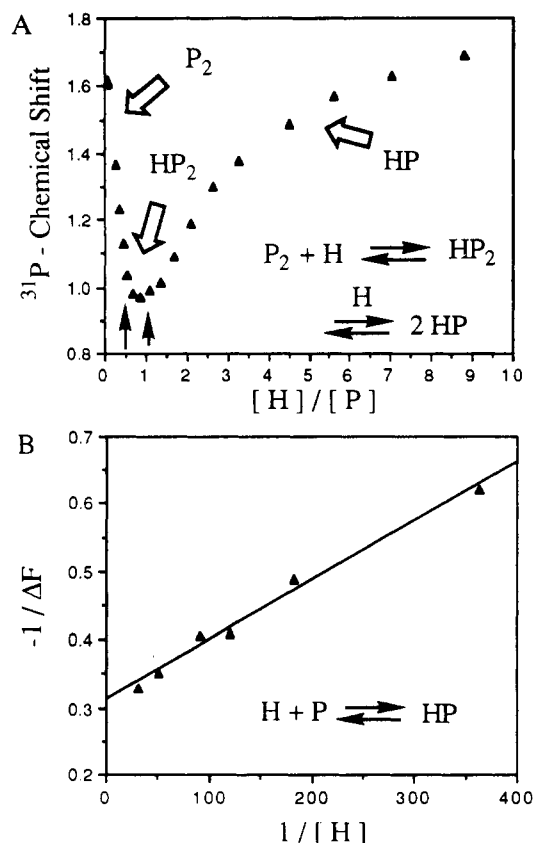


Figure 3. (A) Experimental points following the ^{31}P NMR resonance of dibenzyl phosphate with incremental increases in the concentration of pyridine (H). Concentration of dibenzyl hydrogen phosphate was $2.7 \times 10^{-2}\text{M}$. P = dibenzyl hydrogen phosphate. (B) Double reciprocal plot of total emission intensity of dinaphthyl hydrogen phosphate vs concentration of pyridine. Concentration of dinaphthyl hydrogen phosphate was $1.86 \times 10^{-6}\text{M}$.

of pyridine to 1, 2, and 3 as a means of determining the energy imparted by the addition of hydrogen bond donors and acceptors (see section E).

Figure 3A displays the ^{31}P NMR isotherm generated by maintaining a constant dibenzyl hydrogen phosphate concentration and increasing the pyridine concentration. The ^{31}P resonance first shifts upfield until approximately 0.5 equiv of pyridine has been added; then an inflection occurs, and the resonance moves downfield. After 3–4 equiv of pyridine have been introduced, the chemical shift shows indications of reaching a constant value, but at even 10 equiv of pyridine, a constant chemical shift was not achieved. This isotherm is indicative of both 1:1 and 2:1 phosphoric acid to pyridine binding with a relatively weak 1:1 binding constant.^{14b}

The binding properties of receptors 1–3 were also explored using ^{31}P NMR. As shown in Figure 4A, the ^{31}P NMR isotherm of dibenzyl hydrogen phosphate with 3 resembles that of pyridine. In fact, as shown in Figure 5A, even full cleft 1 yields similar behavior, but the isotherm does reach a plateau near 2–3 equiv, indicating a larger 1:1 association constant.^{14b} In contrast, the isotherm generated with 2 and dibenzyl hydrogen phosphate is indicative of very strong 1:1 binding, with very little evidence of 2:1 guest-to-host binding (Figure 6A). Thus, the behavior of 2 was significantly different from that of 1, 3, and pyridine. Likewise, addition of dibenzyl hydrogen phosphate to a CDCl_3 solution of receptor 2 gave a ^1H binding isotherm showing a sharp break at a host-to-guest ratio of 1:1. Further addition of dibenzyl hydrogen phosphate indicated weak formation of a 2:1 guest-to-host complex (Figure 6B). Thus, the NMR binding isotherms indicate that the strength of complexation of dibenzyl hydrogen phosphate increases in the order pyridine < 3 < 1

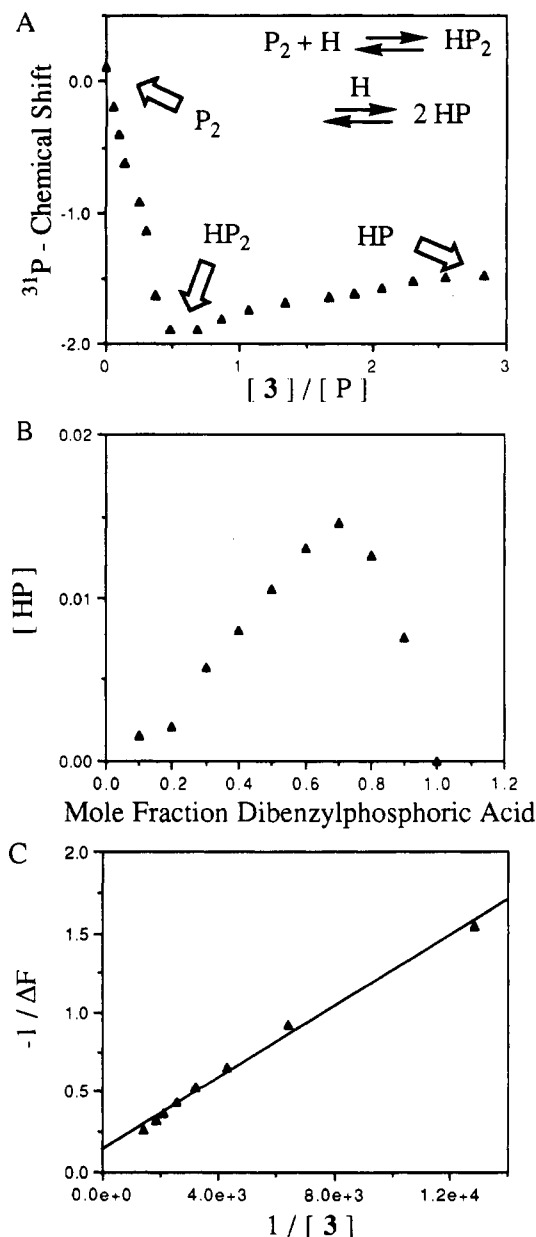
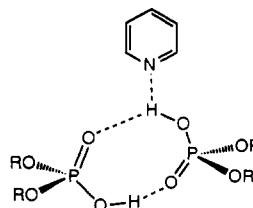


Figure 4. (A) Experimental points following the ^{31}P NMR resonance of dibenzyl hydrogen phosphate (P) with incremental increases in the concentrations of 3 (H). Concentration of dibenzyl hydrogen phosphate was $5.32 \times 10^{-2}\text{M}$. P = dibenzyl hydrogen phosphate. (B) Job plot of the association between dibenzyl hydrogen phosphate and 3. (C) Double reciprocal plot of total emission intensity of dinaphthyl hydrogen phosphate vs concentration of 3. Concentration of dinaphthyl hydrogen phosphate was $2.5 \times 10^{-6}\text{M}$.

< 2. The inflections in the isotherms, however, complicate the determination of binding constants and an analysis of the energetic contributions of the hydrogen bonds.

The inflections in each of the ^{31}P isotherms (except that of 2 and dibenzyl hydrogen phosphate are indicative of 2:1 guest-to-host complexes forming near 0.5 equiv of host. A possible structure for such a complex is shown below with pyridine as an example.



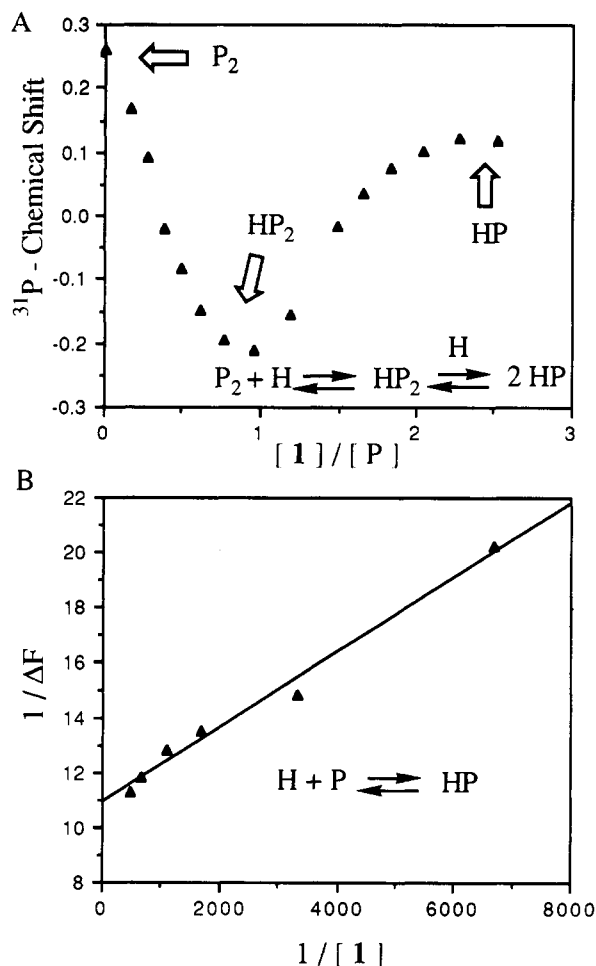
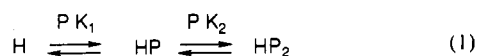


Figure 5. (A) Experimental points following the ^{31}P NMR resonance of dibenzyl hydrogen phosphate (P) with incremental increases in the concentration of 1 (H). Concentration of dibenzyl hydrogen phosphate was 1.8×10^{-2} M. (B) Double reciprocal plot of absorption of 1 vs concentration of 1. Concentration of dibenzyl hydrogen phosphate was 8.0×10^{-6} M.

Due to the presence of excess dibenzyl hydrogen phosphate early in the titration, HP_2 is the first species formed, and when >1 equiv of host is added, the HP complex dominates. In order to confirm the 2:1 binding behavior, a Job plot²³ with host 3 and dibenzyl hydrogen phosphate was performed. Figure 4B was constructed by plotting the complex concentration versus the mole fraction of phosphate. The maximum complex concentration occurred at a dibenzyl hydrogen phosphate mole fraction near 0.67, indicating a stoichiometry of 2:1. Further support for 2:1 complexes are low-temperature NMR studies performed by Denisov and Golubev in chloroform.²⁴ They found that, in a solution containing $(\text{CD}_3)_3\text{N}$ plus a great excess of phosphoric acid diester, all of the amine was involved in a 2:1 phosphoric acid diester to amine complex.

There are two ways in which 2:1 guest-to-host complexes can arise. First, the complexes could arise by formation of a 1:1 complex followed by a strong association of a second phosphoric acid diester (eq 1). A second scenario that would form 2:1



complexes is strong dimerization of the dibenzyl hydrogen phosphate, with which the hosts have to compete to form 1:1 complexes (eq 2). The mathematics that model each of these chemical scenarios are quite different. The algorithms that model

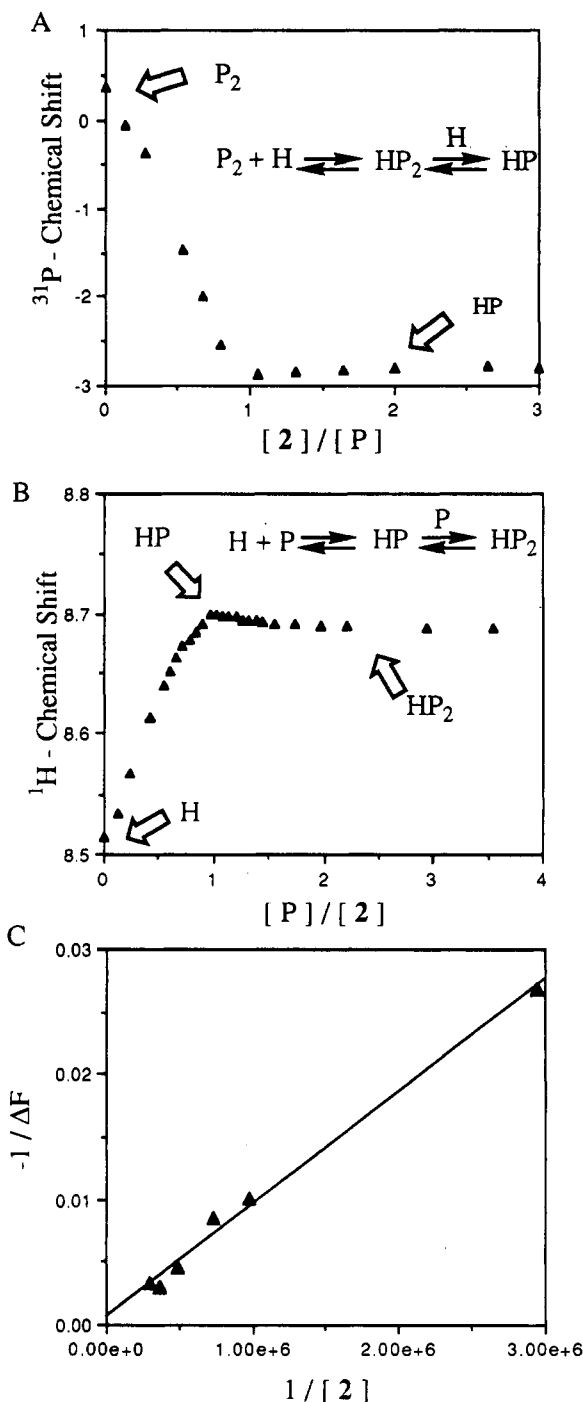
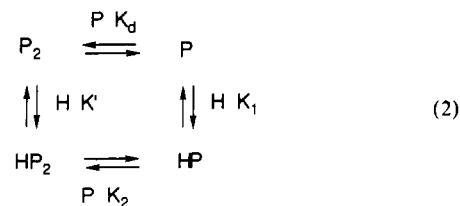


Figure 6. (A) Experimental points following the ^{31}P NMR resonance of dibenzyl hydrogen phosphate (P) with incremental increases in the concentration of 2 (H). Concentration of dibenzyl hydrogen phosphate was 1.17×10^{-2} M. (B) Experimental points following the ^1H NMR resonance of the para pyridine proton of 2 (See Figure 1) with incremental increases in the concentration of dibenzyl hydrogen phosphate. Concentration of 2 was 5.9×10^{-3} M. (C) Double reciprocal plot of total emission intensity of 2 vs concentration of 2. Concentration of dibenzyl hydrogen phosphate was 1.2×10^{-7} M.



solely 1:1 and 2:1 binding (eq 1) have been discussed previously,

(24) Denisov, G. S.; Golubev, N. S. *J. Mol. Struct.* **1981**, 75, 311–326.

and such algorithms can successfully model isotherms similar to those in Figures 3A, 4A, and 5A.¹³ However, eq 1 is not valid if phosphoric acid diester dimerization is occurring. In that case the binding scenario becomes cyclic (eq 2), and the resulting algorithm describing the observed chemical shift is too complex for adequate modeling.²⁵ If phosphoric acid diester dimerization is occurring, one could lower the concentration of the phosphoric acid diester below its dissociation constant, and eq 1 would be valid. A determination of the phosphoric acid dimerization constant was required to delineate if eq 1 or 2 was appropriate for modeling the ³¹P NMR isotherms.

iii. Determining Phosphodiester Dimerization. The presence of phosphoric acid dimers in low dielectric media is supported by cryoscopic studies as well as IR and NMR spectroscopy.²⁶ The dimerization constant of dibutyl hydrogen phosphate in wet chloroform was measured by a distribution study²⁷ and found to be $3.02 \times 10^4 \text{ M}^{-1}$. No dimerization constants, however, were determined for dry chloroform.

To determine a phosphoric acid diester dimerization constant in dry chloroform, a fluorescence titration was performed by the addition of dibenzyl hydrogen phosphate to dinaphthyl hydrogen phosphate. Naphthalene has a high emission intensity in the 310–500-nm wavelength range,²⁸ whereas dibenzyl hydrogen phosphate has negligible emission in this range. Addition of dibenzyl hydrogen phosphate to dinaphthyl hydrogen phosphate caused the emission intensity of dinaphthyl hydrogen phosphate to increase. To perform this study, however, we needed to be confident that the majority of the dinaphthyl hydrogen phosphate was not already dimerized before addition of the dibenzyl probe. Wilcox has shown that the addition of water to chloroform often decreases binding constants of hydrogen-bonding receptors by only 2–3-fold.²⁹ Thus, we estimated a dimerization constant in the range 6.0×10^4 to $9.0 \times 10^4 \text{ M}^{-1}$ on the basis of the dibutyl phosphate dimerization in wet chloroform. The fluorescence titration was therefore performed using a $8.6 \times 10^{-7} \text{ M}^{-1}$ solution of dinaphthyl hydrogen phosphate. A dimerization constant of near 10^6 would be required to significantly aggregate the phosphoric acid at these concentrations, and on the basis of the estimates from the Wilcox studies, this seemed unlikely.

A double-reciprocal plot of the change of emission intensity of dinaphthyl hydrogen phosphate vs concentration of dibenzyl hydrogen phosphate gave a straight line (Figure 7). The dimerization constant (K_d) was measured to be $6.5 \times 10^4 \text{ M}^{-1}$. Control experiments were also performed on pure naphthalene, which, in contrast to dinaphthyl hydrogen phosphate, had no emission intensity change upon the addition of dibenzyl hydrogen phosphate. Therefore, phosphoric acids are strongly aggregated

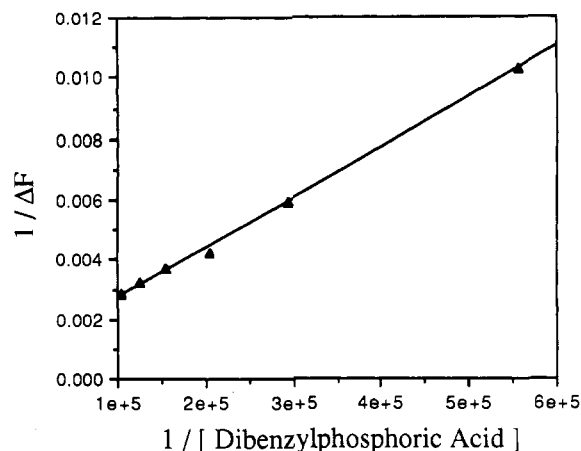
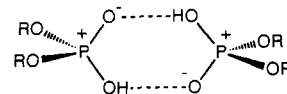


Figure 7. Double reciprocal plot of total emission intensity of dinaphthyl hydrogen phosphate vs the concentration of dibenzyl hydrogen phosphate. Concentration of dinaphthyl hydrogen phosphate was $8.6 \times 10^{-7} \text{ M}$.

in dry chloroform, and the cyclic binding scenario in eq 2 is most appropriate for the NMR isotherms. Simplifying the solution equilibrium to that shown in eq 1 would require a concentration of phosphoric acid diester significantly below $1/K_d$ ($1.5 \times 10^{-5} \text{ M}$), which is impractical for NMR studies.

A dimerization constant between 10^4 and 10^5 M^{-1} for binding involving only two hydrogen bonds is unexpectedly large. In comparison, carboxylic acids dimerize in chloroform with dimerization constants near 500 M^{-1} .³⁰ The exceptionally strong aggregation of the phosphoric acid esters is likely due to their highly acidic nature and the strong dipole in the P–O double bond.



iv. Fluorescence Quenching and UV Binding Studies. Since the NMR titrations as shown in Figures 3A, 4A, 5A, and 6A involve isotherms whose algorithms are too complex for adequate computer modeling²⁵ and phosphoric acid diester concentrations that simplify the algorithms are too dilute to be practical for NMR studies, another analytical technique was required to measure K_1 . Such low concentrations can be readily probed by fluorescence or UV/vis spectroscopy. Indeed, UV/vis spectroscopy has been used previously for measuring binding constants of phosphoric acid diesters to synthetic receptors.³¹

The K_1 values for complexation of pyridine and 1–3 with a phosphoric acid diester were determined by application of the Benesi–Hildebrand equation to fluorescence or UV/vis isotherms (eq 3).³² For example, addition of pyridine to a solution of dinaphthyl hydrogen phosphate in chloroform resulted in a hyperbolic decrease in fluorescence intensity. The double-reciprocal plot gave a binding constant of $3.6 \times 10^2 \text{ M}^{-1}$ (Figure 3B). The same quenching effect was seen upon addition of receptor 3 to a dinaphthyl hydrogen phosphate solution. A binding constant of $1.3 \times 10^3 \text{ M}^{-1}$ was obtained (Figure 4C).

(25) In a cyclic equilibrium the combination of three of the equilibrium constants will yield the fourth, but there is no such interdependence of the δ_{P1} , δ_{P2} , δ_{HP} , and δ_{HP2} . Only δ_{P2} can be measured independently by examination of the ³¹P resonance of pure dibenzyl phosphate in chloroform. Furthermore, we could only independently measure K_d (described herein) and K_1 (described herein). The algorithm for such a scheme, however, has been solved, see: Wyman, J.; Gill, S. J. *Binding and Linkage: Functional Chemistry of Biological Macromolecules*; University Science Books: Mill Valley, CA, 1990.

(26) Corbridge, D. E. C. *The Structural Chemistry of Phosphorus*; Elsevier: New York, 1974; p 247. Peppard, D. F.; Ferraro, J. R.; Mason, G. W. *J. Inorg. Nucl. Chem.* **1959**, *12*, 60. Greenfield, B. F.; Hardy, C. J. *J. Inorg. Nucl. Chem.* **1961**, *21*, 359–365. Peppard, D. F.; Ferraro, J. R.; Mason, G. W. *J. Inorg. Nucl. Chem.* **1961**, *16*, 246–256. Dyrssen, D.; Hay, L. D. *Acta Chem. Scand.* **1960**, *14*, 1091. Hardy, C. J.; Scargill, D. *J. Inorg. Nucl. Chem.* **1959**, *11*, 128–143. Kosolapoff, G. M.; Powell, J. S. *J. Chem. Soc.* **1950**, 3535–3538. Katzin, L. I.; Mason, G. W.; Peppard, D. F. *Spectrochim. Acta* **1978**, *34A*, 51–56. Courtemanche, P.; Merlin, J.-C. *Bull. Soc. Chim. Fran.* **1967**, 3911. Ferraro, J. R.; Peppard, D. F. *J. Phys. Chem.* **1963**, *67*, 2639.

(27) Dyrssen, D. *Acta Chem. Scand.* **1957**, *11*, 1771–1786. Peppard, D. F.; Ferraro, J. R.; Mason, G. W. *J. Inorg. Nucl. Chem.* **1958**, *7*, 231–244. Peppard, D. F.; Ferraro, J. R.; Mason, G. W. *J. Inorg. Nucl. Chem.* **1961**, *22*, 285–291. Dyrssen, D.; Hay, L. D. *Acta Chem. Scand.* **1960**, *14*, 1091–1099.

(28) Emert, J.; Kodali, D.; Catena, R. *J. Chem. Soc., Chem. Commun.* **1981**, 758–759. Arad-Yellin, R.; Eaton, D. F. *J. Phys. Chem.* **1983**, *87*, 5051–5054. Itoh, M.; Fujiwara, Y. *Bull. Chem. Soc. Jpn.* **1984**, *57*, 2261–2265.

(29) Adrian, J. C.; Wilcox, C. S. *J. Am. Chem. Soc.* **1991**, *113*, 678–680.

(30) Brown, C. P.; Mathieson, A. R. *J. Phys. Chem.* **1954**, *58*, 1057–1059. Takeda, K.; Yamashita, H.; Akiyama, M. *Solvent Extr. Ion Exch.* **1987**, *5*, 29–53. Maciel, G. E.; Traficante, D. D. *J. Am. Chem. Soc.* **1966**, *88*, 220–223. Harris, J. T., Jr.; Hobbs, M. E. *J. Am. Chem. Soc.* **1954**, *76*, 1419–1422. I'Haya, Y.; Shibuya, T. *Bull. Chem. Soc. Jpn.* **1965**, *38*, 1144–1147. Barrow, G. M.; Yenger, E. A. *J. Am. Chem. Soc.* **1954**, *76*, 5248–5249.

(31) Hirst, S. C.; Tecilla, P.; Geib, S. J.; Fan, E.; Hamilton, A. D. *Isr. J. Chem.* **1992**, *32*, 105.

(32) Benesi, H. A.; Hildebrand, J. H. *J. Am. Chem. Soc.* **1949**, *71*, 2703–2707. Alvarez, R.; Carmona, E.; Marin, J. M.; Povada, M. L.; Gutierrez-Puebla, E.; Monge, A. *J. Am. Chem. Soc.* **1986**, *108*, 2286–2294.

$$1/\Delta F = 1/(C_S K k_d C_L) + 1/(C_L k_d) \quad (3)$$

ΔF : the fluorescence intensity change upon addition of the guest
 C_S : total host concentration
 C_L : total guest concentration

Receptor **2** has an intense fluorescence band at 415–600 nm ($\lambda_{\text{max}} = 457$ nm), but no fluorescence of dibenzyl phosphate was observed in this range. Upon addition of dibenzyl hydrogen phosphate, the fluorescence intensity of **2** was decreased. Since the concentration of dibenzyl hydrogen phosphate must be kept below its dissociation constant, an experiment was performed following the fluorescence of receptor **2** while changing its concentration and keeping the dibenzyl hydrogen phosphate concentration constant (Figure 6C). The Benesi–Hildebrand equation can be applied to the fluorescence of either the compound whose concentration is held constant or the one whose concentration is varied (supplementary material). The ΔF in Figure 6C is the difference in emission intensity between a solution containing C_S of receptor **2** with dibenzyl hydrogen phosphate, and a similar solution lacking dibenzyl hydrogen phosphate. This treatment of the fluorescence difference between the two solutions gave a binding constant of $8.9 \times 10^4 \text{ M}^{-1}$.

UV/vis absorption was used to measure the binding constant of dibenzyl hydrogen phosphate with **1**. Upon addition of guest to solutions of **1**, the absorption intensity at 436 nm increases. Dibenzyl hydrogen phosphate does not absorb at this wavelength. The UV/vis change may be indicative of proton transfer from the phosphate to the guest, as found in similar systems.³¹ The existence of a positive charge on **1**, however, would tend to disfavor such a proton transfer. Figure 5B shows a double-reciprocal plot of the change in absorbance of **1**, caused by the presence of dibenzyl hydrogen phosphate, vs concentration of **1**. The change in absorption was measured by subtracting the absorption of solutions containing receptor **1** with and without dibenzyl hydrogen phosphate. Application of the Benesi–Hildebrand method gave a binding constant of $7.8 \times 10^3 \text{ M}^{-1}$.³³ Thus, the subtle difference between receptor **1** and **2** resulted in significantly different binding constants: 7.8×10^3 vs 8.9×10^4 .

D. Structural Studies. To probe how the structural differences between receptors **1** and **2** resulted in different binding constants, molecular mechanics calculations were performed.³⁴ We have shown before that molecular mechanics finds the structures of rigid hosts such as **1** to be almost identical with the corresponding crystal structures.³⁵ The calculations with a docked dimethyl hydrogen phosphate revealed four hydrogen bonds with the receptors (Figure 8). The hydrogen bond lengths between the heteroatoms in the calculated host–guest structures were all between 2.7 and 3.0 Å, within the optimum hydrogen-bonding distance of 2.8–3.2 Å.³⁶ The angles deviated from linearity by between 10° and, at an extreme, 20° . The bond angles in the dimethyl hydrogen phosphate–receptor **2** complex, however, were on average 8° closer to linearity than those in the receptor **1** complex. The molecular mechanics calculations therefore suggest that the difference in binding constants of phosphoric acid diesters with **1** and **2** are due to differences in hydrogen bond angles. These angle differences derive from the different linkers

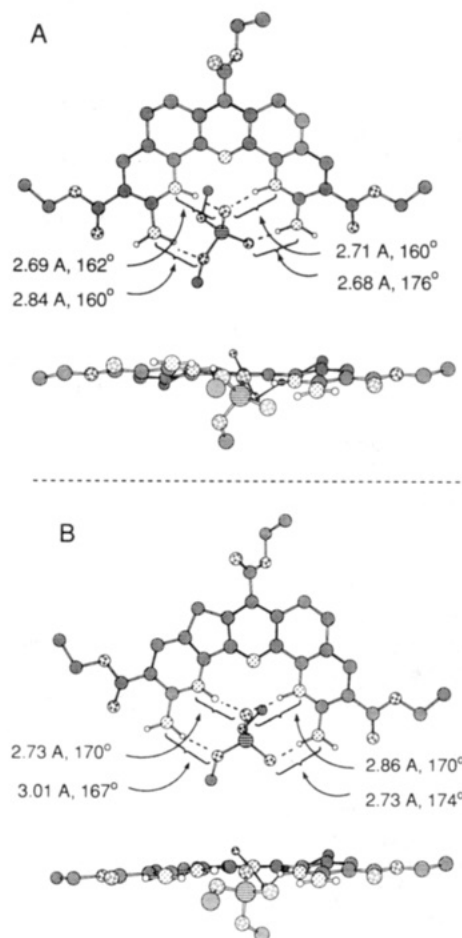


Figure 8. Molecular mechanics calculated structures for the complexation of dimethyl hydrogen phosphate with (A) **1** and (B) **2**.

between the pyridines of **1** and **2**. The two ethanediyl linkers of **1** form a smaller cavity than that in **2**.

Support for a connection between the binding constant differences found for **1** and **2** with the size of the cavity can be gleaned from analysis of other spacers. The ethanediyl linkers of **1** place the pyridine and amine hydrogen-bonding contacts in similar spatial positions, as does the isophthaloyl spacer in receptor **20** (Figure 9).³⁷ Hamilton has reported that the isophthaloyl spacer forms a cleft which is slightly too narrow for a barbiturate, since a crystal structure of **20** revealed the guest displaced from the cavity by about 27° .³⁸ In comparison, Thummel has reported the complexation of urea derivatives using receptor **21**. This receptor possesses a cavity slightly larger (Figure 9) than that of **20** or **1**, and a crystal structure of **21** with imidazolidone found the guest in the plane of the receptor.³⁹

In order to compare the size of the cavities in **1**, **2**, **20**, and **21** with their binding properties, one must first analyze the size of their respective guests. The distances between the hydrogen bond donors and acceptors of a phosphoric acid diester are larger than those in a barbiturate or a urea. The phosphorus(V) atom has an atomic radius of 34 pm compared to the carbon(IV) radius of 15 pm.⁴⁰ This is reflected in the bond lengths; barbiturate C–N bonds are typically near 1.35 Å,^{41a} and phosphate P–OR bonds are typically near 1.6 Å.^{41b} Thus, the larger central atom in the phosphodiester causes the distance between the four phosphate oxygens (2.57 Å) to be larger than the distance between

(33) In all the binding studies the boundary conditions for the Benesi–Hildebrand treatment have been followed. First of all, the concentration of the species that is varied was always in very large excess over the minor component, typically by a factor of 10^3 or more. Also, Bergeron showed that if the concentration of the minor component is greater than one-tenth the K_a , then large errors are introduced using the Benesi–Hildebrand treatment. Note that in each of our studies the concentration of the minor component is always less than one hundredth of $1/K(K_a)$. Bergeron, R. J.; Roberts, W. P. *Anal. Biochem.* **1978**, *90*, 844–848.

(34) Still, C. *MACROMODEL* Version 2.5, Columbia University.

(35) Huang, C.-Y.; Lynch, V.; Anslyn, E. V. *Angew. Chem., Int. Ed. Engl.* **1992**, *31*, 1244.

(36) Jeffrey, G. A.; Saenger, W. *Hydrogen Bonding in Biological Structures*; Springer Verlag: New York, 1991.

(37) Chang, S.-K.; Van Engen, D.; Fan, E.; Hamilton, A. D. *J. Am. Chem. Soc.* **1988**, *110*, 1318–1319.

(38) Chang, S.-K.; Van Engen, D.; Fan, E.; Hamilton, A. D. *J. Am. Chem. Soc.* **1991**, *113*, 7640–7645.

(39) Hegde, V.; Hung, C.-Y.; Madhukar, P.; Cunningham, R.; Hopfner, T.; Thummel, R. P. *J. Am. Chem. Soc.* **1993**, *115*, 872–878.

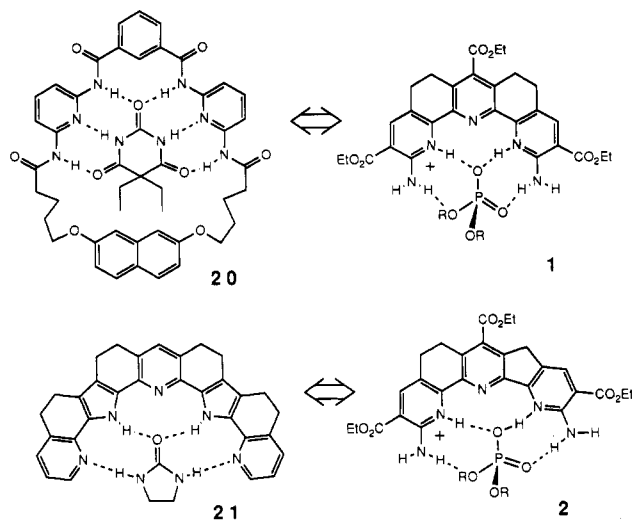


Figure 9. Isophthalaloyl (20) and terpyridine (1) spacers have smaller cavities than 21 and 2.

Table 1. Complexation Constants and Free Energies for Pyridine and 1–3, with either Dibenzyl Hydrogen Phosphate or Dinaphthyl Hydrogen Phosphate

| receptor | guest | K_a (M^{-1}) | ΔG (kcal/mol) |
|----------|-------------------------------|--------------------|-----------------------|
| pyridine | dinaphthyl hydrogen phosphate | 3.6×10^2 | -3.48 |
| 3 | dinaphthyl hydrogen phosphate | 1.3×10^3 | -4.25 |
| 1 | dibenzyl hydrogen phosphate | 7.8×10^3 | -5.31 |
| 2 | dibenzyl hydrogen phosphate | 8.9×10^4 | -6.75 |

the barbiturate urea-like nitrogens (2.23 Å) even though the barbiturate bond angles are larger. Since a phosphoric acid diester is larger than a barbiturate and an isophthalaloyl-based cavity is too small for ideal barbiturate binding, clearly a similar cavity (as in 1) would be far too small for a phosphodiester. Hence, a wider cavity as in receptor 2 should be more complementary for hydrogen bonding to phosphodiesters than those based upon or modeled after the isophthalaloyl spacer. In the experiments discussed herein, the binding advantage imparted by widening the cavity was 1.4 kcal/mol (Table 1).⁴²

E. Energetic Analysis. By comparing the binding constants of phosphoric acid diesters with those of 1–3 and pyridine, one can extract the incremental increase in binding imparted by the hydrogen-bonding groups. The energy of complexation between pyridine and dinaphthyl hydrogen phosphate is 3.5 kcal/mol (Table 1). This is quite a large complexation constant for just one hydrogen bond, given that translational entropy was reduced during this association. This undoubtedly arises from the highly acidic nature of phosphoric acids. Further hydrogen bond formation as with 3 (Scheme 1), results in an additional 0.77 kcal/mol. Thus, the second hydrogen bond between the amino group of 3 and the phosphoryl oxygen is significantly weaker than the hydrogen bond between pyridine and phosphoric acid. We cannot currently rule out the possibility that the 0.77 kcal/mol increase is solely due to the greater basicity of 3 vs pyridine. Further analysis of Table 1 again reveals that the additional hydrogen bonds with 1 and 2 are weaker than that between pyridine and dinaphthyl hydrogen phosphate. They are weaker

even though one of the hydrogen bonds is cationic. The energetic advantage of binding a phosphoric acid diester with 1 or 2 over 3 is 1.06 or 2.5 kcal/mol, respectively. Therefore, the additional hydrogen bonds formed with 1, 2, or 3 are all weaker than that formed between the most acidic guest donor and the most basic host acceptor. The concept that the most acidic donating group pairing with the most basic accepting group yields the most exothermic binding interaction is similar to what has been found in solid-state crystal lattices. Etter has described that the hydrogen-bonding arrays in crystalline lattices can be predicted by first pairing the best donor and acceptor, followed by pairing the weaker donors and acceptors.⁴³ The results given in Table 1 support a similar predictive strategy for host–guest complexes in solution.

One advantage of studying molecular recognition processes with rigid polyaza-clefts is the capability to incrementally add hydrogen-bonding groups in a preorganized fashion and thus analyze the energies of individual molecular recognition contacts, as discussed above. Similar analyses with other receptors have been performed. For example, both Hamilton⁴⁴ and Schneider⁴⁵ have found that hydrogen bonds between urea-like O's and amide-like NH's are worth roughly 1.2 kcal/mol in chloroform. The binding difference between 2 and 3, involving a change of two hydrogen bonds, is 2.5 kcal/mol. One of these two additional hydrogen bonds is between a phosphoester OR acceptor and an aromatic amine NH donor. This hydrogen bond is likely similar in strength to the additional hydrogen bond formed with 3 vs pyridine (near 0.8 kcal/mol). The second additional hydrogen bond is formed between a pyridinium donor and a phosphoester OH acceptor. Thus, we can estimate the strength of this hydrogen bond to be near 1.7 kcal/mol. Alternatively, if it is assumed that each of the two hydrogen bonds are similar in strength, then they are worth nearly 1.25 kcal/mol. With either interpretation, the values are similar to those found by Hamilton and Schneider. This similarity is intriguing, since hydrogen bond strengths should be quite sensitive to microenvironment, as discussed by Thummel. Thummel has found that hydrogen bond strengths respond to factors such as the Lewis acid/base nature of the partners and the organization of the system.⁴⁶ Most intriguing is that the pyridinium hydrogen bond donor yields a hydrogen bond strength similar to that for a neutral donor. In contrast, in other studies we have found that charged hydrogen bonds lead to substantial increases in free energy of complexation in methylene chloride.⁴⁷ In the case of 2, however, the existence of a positive charge likely significantly depresses the basicity of the second pyridine nitrogen, so that the hydrogen bonding between this pyridine and dibenzyl hydrogen phosphate is weaker than that measured for dinaphthyl hydrogen phosphate and pyridine. Thus, it is apparent that the strengths of hydrogen bonds are dependent upon the nature of the partners, the structural matching between the host and guest, as well as the microenvironment around the hydrogen bonds.

Conclusions

The NMR binding isotherms of dibenzyl hydrogen phosphate with pyridine and receptors 1–3 all indicate 2:1 and 1:1 guest-to-host complexes. The highly acidic nature of phosphoric acid esters and their strong tendency to dimerize in nonpolar solvents result in complexes with higher than 1:1 stoichiometry with synthetic receptors. Similar effects may also complicate

(40) Huheey, J. E. *Inorganic Chemistry: Principles of Structure and Reactivity*, 2nd ed.; Harper & Row: New York, 1978; p 71.

(41) (a) Blessing, R. H. *J. Am. Chem. Soc.* **1983**, *105*, 2776–2783. (b) Dobrowolska, W. S. *Acta Crystallogr.* **1987**, *C43*, 1944–1946. Poutasse, C. A.; Day, R. O.; Holmes, R. R. *J. Am. Chem. Soc.* **1984**, *106*, 3814–3820. Yoo, C. S.; Wood, M. K.; Sax, M.; Pletcher, J. *Acta Crystallogr.* **1975**, *B31*, 1354–1360. Perales, A.; Garcia-Blanco, S. *Acta Crystallogr.* **1978**, *B34*, 238–242.

(42) In water, we have reported that a wider "bis-guanidinium" cleft does not show stronger binding than a cleft patterned after an isophthalaloyl spacer.^{16b} This is likely due to increased flexibility with these "bis-guanidinium" receptors. A completely neutral wider receptor, however, does show strong binding in acetonitrile, see: Anslyn, E. V.; Smith, J.; Kneeland, D. M.; Ariga, K.; Chu, F. *Supramolecular Chem.* **1993**, *1*, 201–208.

(43) Etter, M. C. *Acc. Chem. Res.* **1990**, *23*, 120–126.

(44) Vicent, C.; Fan, E.; Hamilton, A. D. *Tetrahedron Lett.* **1992**, *33*, 4269.

(45) Schneider, H.-J.; Juneja, R. K.; Simova, S. *Chem. Ber.* **1989**, *122*, 1211.

(46) Hung, C.-Y.; Höpfner, T.; Thummel, R. P. *J. Am. Chem. Soc.* **1993**, *115*, 12601.

(47) Bell, D.; Anslyn, E. V. *J. Org. Chem.* **1994**, *59*, 512–514.

synthetic receptors for carboxylic acids in chloroform.⁴⁸ Indeed, 2:1 complexes between carboxylic acids and simple amines have been reported previously.⁴⁹ Such dimerization should also affect transport studies. The transport of phosphodiester through lipophilic media may commonly involve complexes of stoichiometry greater than 1:1. In support of this, crystal structures of phosphate receptors from the Sessler group⁵⁰ revealed one phosphate bound and another phosphate associated with the first phosphate.

The strongest binding interaction between phosphoric acid diesters and pyridine-based hosts such as those described herein is between the phosphoric acid hydrogen and the pyridine nitrogen. The additional hydrogen bonds formed between receptors 1–3 and the phosphoric acid diesters are significantly weaker. Modifying the structure of receptor 1 to yield 2 resulted in a wider cleft and increased binding by 1.5 kcal/mol. Thus, cavities wider than that in 1 can lead to better positioning of hydrogen bond donors and acceptors for complementary interactions to phosphodiester.

Experimental Section

A. General Considerations. The ¹H NMR titrations were performed on a Bruker ACF-250 NMR spectrometer. ³¹P NMR titrations were performed on a Nicolet NT-360 NMR spectrometer. An internal capillary tube containing the reference triphenylphosphine was used in each ³¹P NMR study. UV/vis Beer's law plots were generated on a Beckman DU-70 spectrophotometer. Fluorescence quenching studies were performed on a SPF-500 C spectrometer. All solvents for analytical studies were dried by stirring with CaH₂, distilled, and stored in a Vacuum Atmosphere MO-20 drybox.

Compounds 1,¹⁹ 3,¹⁹ 4,⁵¹ 5,⁵² and 10,^{20,53} ethyl glyoxlate,⁵⁴ and sodium tetrakis(3,5-bis(trifluoromethyl)phenyl)borate¹⁷ were synthesized following literature procedures.

B. Beer's Law Studies. The concentrations of the host and guest solutions used in the binding studies were determined from their UV absorbances at λ_{max} and applying Beer's law. Generally six concentration points were taken for each Beer's law graph. A correlation constant of 0.997 or better was obtained for each graph. The extinction coefficients for 1, 2, and 3 were 29 025, 26 150, and 14 090 M⁻¹cm⁻¹, respectively, and the λ_{max} values were 436, 421, and 379.5 nm, respectively.

C. NMR Binding Studies. The NMR binding studies were performed by three different procedures: (1) The ³¹P NMR experiments used a constant guest concentration. (2) The ¹H NMR experiments used variable host and guest concentrations. (3) The Job plot used a constant total concentration of host plus guest.

Procedure 1 was performed by preparing 2 mL of a guest stock solution. The host was weighed in an NMR tube (the concentration was checked by UV/vis spectroscopy), and 0.5 mL of the guest stock was added. The initial NMR sample had host at several times higher concentration than guest. For subsequent NMR measurements, volumes of solution were removed from the NMR tube and replaced with equal volumes of the guest stock solution, thus incrementally diluting the host concentration but retaining constant guest concentration.

Procedure 2 was performed by adding measured volumes of a highly concentrated guest stock solution to an NMR sample containing the desired concentration of host. In this manner the guest concentration

was incrementally increased while the host concentration remained essentially the same.

Procedure 3 was performed by preparing an initial NMR sample pure in host and a stock solution pure in guest, both at equimolarity. The concentrations were checked by UV/vis spectroscopy and adjusted until equal. Measured volumes of solution were then removed from the NMR tube and replaced with equal volumes of the guest solution. This procedure was continued until the contents of the NMR tube had been switched to almost completely pure guest.

D. Fluorescence Binding Studies. The binding constants were obtained by applying the Benesi–Hildebrand method in which ΔF was obtained by two different procedures. In order to avoid guest dimerization, the concentration of dibenzyl hydrogen phosphate was kept below the dissociation constant. Due to the low quantum yield of dibenzyl hydrogen phosphate, however, the fluorescence cannot be detected at such concentrations. Therefore, two procedures were developed, one which followed the fluorescence of the host (procedure I) and one using a more fluorescent guest dinaphthylphosphoric acid (procedure II).

Procedure I: Two stock solutions were prepared in chloroform, one of host and a second of guest. The host stock solution was much more concentrated than the guest stock solution. F_0 values were obtained by adding different volumes of host stock solution to a set volume of chloroform in a quartz cell. F values were obtained by adding the same aliquots of the host stock solution as in measuring F_0 , except to a set volume of guest stock solution. From the intercept and slope of the plot of $1/\Delta F$ ($\Delta F = F - F_0$) vs $1/[H]$ (eq 3) the binding constants were calculated, $K = \text{slope/intercept}$. Procedure II: Dibenzyl hydrogen phosphate and dinaphthyl hydrogen phosphate stock solutions were prepared and the concentrations determined by UV/vis absorbance. A fluorescence cell was loaded with dinaphthyl hydrogen phosphate stock solution and degassed, and a spectrum was recorded to obtain F_0 (exciting the dinaphthyl hydrogen phosphate, $\lambda_{\text{excitation}} = 286$ nm, emission between 320 and 350 nm). To this solution, dibenzyl hydrogen phosphate stock solution was added several times to obtain F values. Each resulting solution was mixed thoroughly, and the dinaphthyl hydrogen phosphate emission spectrum was recorded.

Binding constants of dinaphthyl hydrogen phosphate to pyridine and receptor 3 were obtained by the same method. ΔF was the difference of emission intensity integral between 340 and 350 nm for pyridine and the measure emission at 341 nm for 3. Control studies were done by plotting F_0/F_n vs concentration of quencher (Stern–Volmer). Either a straight line or concave upward curves were obtained, indicating that the quenching phenomena was due solely to static quenching.

E. Synthesis. **2-Benzylidene-6-[(dimethylamino)methylidene]cyclohexanone (6).** A flame-dried 500-mL round-bottom flask was charged with 20 g (0.107 mol) of 2-benzylidene-cyclohexanone, 89.7 g (0.749 mol) of *N,N*-dimethylformamide dimethyl acetal, and 180 mL of dry DMF. The reaction was allowed to reflux for 3.5 h, wherein the light-yellow solution turned dark green. The excess DMF and *N,N*-dimethylformamide dimethyl acetal were removed under vacuum, yielding bright green crystals. The crystals were filtered and then washed with hexanes, yielding 23.5 g of compound 6 (97 mmol, 91%): mp 136–140 °C; ¹H NMR (300 MHz, CDCl₃) δ 7.74 (s, 1H, vinyl), 7.70 (s, 1H, vinyl), 7.33 (m, 5H, Ar), 3.12 (s, 3H, NCH₃), 3.06 (s, 3H, NCH₃), 2.76 (m, 4H, CH₂CH₂), 1.69 (m, 2H, CH₂CH₂CH₂); ¹³C {¹H} NMR (75 MHz, CDCl₃) δ 23.78, 26.02, 28.16, 30.84, 43.38, 105.24, 127.33, 128.01, 129.92, 132.22, 137.04, 137.21, 151.63, 187.31. HRMS *m/z* calcd for C₁₆H₁₉NO 241.1466, obsd 241.1461. 241.1466 Anal. Calcd for C₁₆H₁₉NO: C, 79.63; H, 7.94; N, 5.8. Found: C, 79.76; H, 7.92; N, 5.73.

3-Benzylidene-2-oxocyclohexanecarboxaldehyde (8). To 19 g (0.079 mol) of 6 in an Erlenmeyer flask was added 180 mL of 2 N HCl and 100 mL of CH₂Cl₂. The reaction was allowed to stir overnight. The mixture was then extracted with CH₂Cl₂, dried over MgSO₄, and concentrated, to give 15.9 g of a yellow solid (94%): mp 77–80 °C; ¹H NMR (300 MHz, CDCl₃) δ 14.44 (s, 1H, OH), 9.02 (s, 1H, vinyl), 7.61 (s, 1H, vinyl), 7.34 (m, 5H, Ar), 2.69 (p, 5H, CH₂CH₂CH₂), 2.45 (t, 2H, CH₂), 1.72 (t, 2H, CH₂); ¹³C {¹H} NMR (75 MHz, CDCl₃) δ 23.01, 23.82, 26.64, 109.86, 127.44, 128.18, 128.31, 129.25, 129.95, 131.35, 133.29, 136.04, 171.85, 191.97. HRMS *m/z* calcd for C₁₄H₁₄O₂ 214.0994, obsd 214.0984. Anal. Calcd for C₁₄H₁₄O₂: C, 78.48; H, 6.59. Found: C, 78.53; H, 6.58.

2-[(3,4-Dimethoxyphenyl)methylamino]-8-benzylidene-5,6,7,8-tetrahydroquinoline-3-carboxylic Acid, Ethyl Ester (11). A flame-dried round-bottom flask was charged with 6.2 g (28.9 mmol) of 8 and 120 mL of dry THF. To this was added 7 g (25.1 mmol) of 3-[(3,4-dimethoxyphenyl)methylamino]-3-aminopropenoic acid (10), and the

(48) For recent carboxylic acid receptors see: Fan, E.; Van Arman, S. A.; Kincaid, S.; Hamilton, A. D. *J. Am. Chem. Soc.* **1993**, *115*, 369–370. Garcia-Tellado, F.; Goswami, S.; Chang, S.-K.; Geib, S. J.; Hamilton, A. D. *J. Am. Chem. Soc.* **1990**, *112*, 7393–7394. Rebek, J. Jr.; Nemeth, D.; Ballester, P.; Lin, F.-T.; *J. Am. Chem. Soc.* **1987**, *109*, 3474.

(49) Yenger, E. A.; Barrow, G. M. *J. Am. Chem. Soc.* **1955**, *77*, 6206–6207. Barrow, G. M. *J. Am. Chem. Soc.* **1956**, *78*, 5802–5806. Yenger, E. A.; Barrow, G. M. *J. Am. Chem. Soc.* **1955**, *77*, 4474.

(50) Sessler, J. L.; Cyr, M.; Furuta, H.; Kral, V.; Mody, T.; Morishima, T.; Shionoya, M.; Weghorn, S. *Pure Appl. Chem.* **1993**, *65*, 393–398. Sessler, J. L.; Furuta, H.; Kral, V. *Supramolecular Chem.* **1993**, *1*, 209–220. These papers do not show the second phosphate in the structures; a personal communication from J. L. Sessler, however, confirmed their existence.

(51) Baltzly, R.; Lorz, E.; Russell, P. B.; Smith, F. M. *J. Am. Chem. Soc.* **1955**, *77*, 624–628.

(52) Birkofer, L.; Kim, S. M.; Engels, H. D. *Chem. Ber.* **1962**, 1495–1504.

(53) Meyer, H.; Bossert, F.; Horstmann, H. *Justus Liebigs Ann. Chem.* **1977**, 1895–1908.

(54) Kelly, T. R.; Schmidt, T. E.; Haggerty, J. G. *Synthesis* **1972**, 544–545.

reaction was allowed to stir for 12 h. The solvent was removed by rotary evaporation and the residue purified by silica gel chromatography (hexane/EtOAc = 4:1): yield 7.8 g (58.9%); mp 65–68 °C; ^1H NMR (300 MHz, CDCl_3) δ 8.08 (t, 1H, NH), 8.03 (s, 1H, para pyridine H), 7.88 (s, 1H, C=CHPh), 7.18 (m, 7H, Ar), 6.82 (d, 1H, $\text{C}_6\text{H}_3(\text{OMe})_2$), 4.74 (d, 2H, CH_2Ar), 4.31 (q, 2H, CH_2Me), 3.84 (s, 3H, OCH_3), 3.81 (s, 3H, OCH_3), 2.84 (t, 2H, CCH_2), 2.71 (t, 2H, CCH_2), 1.79 (m, 2H, $\text{CH}_2\text{CH}_2\text{CH}_2$), 1.37 (t, 3H, CH_2CH_3); ^{13}C { ^1H } NMR (75 MHz, CDCl_3) δ 14.27, 23.17, 27.90, 28.57, 44.86, 55.69, 55.81, 60.47, 105.47, 111.10, 119.73, 120.53, 126.88, 128.01, 129.05, 129.63, 132.99, 135.48, 137.68, 140.76, 147.84, 148.84, 155.19, 155.87, 167.32. Anal. Calcd for $\text{C}_{28}\text{H}_{30}\text{N}_2\text{O}_4$: C, 73.34; H, 6.59. Found: C, 73.26; H, 6.62.

2-[(3,4-Dimethoxyphenyl)methyl]amino-8-oxo-5,6,7,8-tetrahydroquinoline-3-carboxylic Acid, Ethyl Ester (13). A round-bottom flask was charged with 6.8 g (14.85 mmol) of **11** dissolved in 85 mL of H_2O and 250 mL of THF. Subsequently 3.03 g (0.297 mmol) of OsO_4 (2.5% solution in 2-methyl-2-propanol) was added and the mixture stirred for 20 min. NaIO_4 (7.9 g, 40 mmol) was then added in portions over 30 min. The mixture was allowed to stir for 24 h. The THF was removed under reduced pressure, water was added to the residue, and it was extracted with CH_2Cl_2 . The combined CH_2Cl_2 layers were washed with sodium bisulfite. After being dried with MgSO_4 , the solution was concentrated on a rotary evaporator. The residue was purified by silica gel chromatography (hexanes/EtOAc = 2:1): yield 4.1 g (72%); mp 114–117 °C; ^1H NMR (300 MHz, CDCl_3) δ 1.38 (t, 3H, CH_2CH_3), 2.13 (m, 2H, $\text{CH}_2\text{CH}_2\text{CH}_2$), 2.74 (t, 2H, $\text{CH}_2\text{CH}_2\text{CH}_2$), 2.87 (t, 2H, $\text{CH}_2\text{CH}_2\text{CH}_2$), 3.85 (s, 3H, OCH_3), 3.88 (s, 3H, OCH_3), 4.33 (q, 2H, CH_2CH_3), 4.71 (d, 2H, CH_2Ar), 7.01 (m, 3H, Ar), 8.10 (s, 2H, NH and para pyridine proton); ^{13}C { ^1H } NMR (75 MHz, CDCl_3) δ 14.14, 22.97, 28.02, 39.96, 44.97, 55.78, 61.21, 111.02, 112.10, 120.34, 127.94, 131.99, 141.89, 148.00, 149.42, 156.57, 166.47, 196.71; HRMS m/z calcd for $\text{C}_{21}\text{H}_{24}\text{N}_2\text{O}_5$: 384.1685, obsd 384.1678. Anal. Calcd for $\text{C}_{21}\text{H}_{24}\text{N}_2\text{O}_5$: C, 65.61; H, 6.29; N, 7.29. Found: C, 65.61; H, 6.30; N, 7.29.

2-[(3,4-Dimethoxyphenyl)methyl]amino-7-(2-ethoxy-2-oxoethylidene)-8-oxo-5,6,7,8-tetrahydroquinoline-3-carboxylic Acid, Ethyl Ester (17). A flame-dried round-bottom flask was equipped with a reflux condenser and a N_2 inlet. The apparatus was charged with 2.3 g (5.99 mmol) of **13** in 80 mL of dry THF. To this was added 80 mg of TsOH and then 2.58 g (17.97 mmol) of 1-(trimethylsilyl)pyrrolidine. The reaction was allowed to stir at 60 °C for 1 h and then at 25 °C overnight. The solvent was removed in vacuo. The residue was checked by ^1H NMR and used for the next reaction without further purification. A round-bottom flask containing the above enamine (2.62 g, 5.99 mmol) was charged with 50 mL of dry THF and cooled to –78 °C. Ethyl glyoxalate (4 equiv) was vacuum flash distilled from P_2O_5 into the above solution using a heat gun. This reaction was allowed to warm to room temperature overnight under N_2 . Then 20 mL of 0.01 N HCl was added and the mixture stirred for 5 h. The solution was extracted with three 50-mL portions of ether and three 50-mL portions of CH_2Cl_2 . The combined organic layers were dried over MgSO_4 , and the solvent was removed by rotary evaporation. The residue was purified by silica gel chromatography (EtOAc/hexanes = 1:2): yield 1.7 g, 61%; mp 106–108 °C; ^1H NMR (300 MHz, CDCl_3) δ 1.36 (m, 6H, CH_2CH_3), 2.30 (t, 2H, CH_2CH_2), 3.43 (m, 2H, CH_2CH_2), 3.86 (s, 3H, OCH_3), 3.89 (s, 3H, OCH_3), 4.26 (q, 2H, CH_2CH_3), 4.34 (q, 2H, CH_2CH_3), 4.72 (d, 2H, CH_2Ph), 7.04 (m, 4H, Ar and C=H), 8.13 (s, 1H, para pyridine proton), 8.16 (t, 1H, NH); ^{13}C { ^1H } NMR (75 MHz, CDCl_3) δ 13.85, 26.02, 26.37, 44.68, 55.51, 60.34, 61.07, 110.32, 110.81, 111.87, 120.09, 123.84, 127.76, 131.60, 141.15, 147.78, 148.52, 149.07, 149.27, 156.54, 165.63, 166.02, 185.14; HRMS m/z calcd for $\text{C}_{25}\text{H}_{28}\text{N}_2\text{O}_7$: 468.1896, obsd 468.1901. Anal. Calcd for $\text{C}_{25}\text{H}_{28}\text{N}_2\text{O}_7$: C, 64.09; H, 6.02; N, 5.98. Found: C, 64.07; H, 6.04; N, 5.96.

2-Benzylidene-5-[(dimethylamino)methylidene]cyclopentanone (7). A dry 250-mL round-bottom flask was charged with 14.2 g (0.083 mol) of 2-(benzylidene)cyclopentanone under an N_2 atmosphere. To this flask was added 76.8 mL of N,N -dimethylformamide dimethyl acetal. The reaction was allowed to stir for 20 h at 40–45 °C. Yellow crystals precipitated. Compound **7** was collected by filtration and purified by recrystallization (CH_2Cl_2 , hexanes). Ice water was added to the filtrate, and the aqueous solution was extracted with CH_2Cl_2 . The organic layer was dried over MgSO_4 and filtered, and the solvent was removed with a rotary evaporator. This residue was purified by crystallization: yield 16.21 g, 86%; mp 207–210.5 °C; ^1H NMR (300 MHz, CDCl_3) δ 2.92 (4H, m, CH_2CH_2), 3.10 (s, 6H, NCH_3), 7.40 (m, 7H, HC=C and Ar); ^{13}C { ^1H } NMR (75 MHz, CDCl_3) δ 24.47, 26.53, 42 (m), 105.99, 127.70, 128.33, 129.79, 136.85, 140.40, 148.07, 193.23. HRMS m/z calcd for

$\text{C}_{15}\text{H}_{17}\text{NO}$ 227.1310, obsd 227.1304. Anal. Calcd for $\text{C}_{15}\text{H}_{17}\text{NO}$: C, 79.26; H, 7.54; N, 6.16. Found: C, 79.15; H, 7.51; N, 6.11.

3-Benzylidene-2-oxocyclopentanecarboxaldehyde (9). A 500-mL round-bottom flask was charged with 8 g (35.2 mmol) of **7**, 90 mL of 2 N HCl, and 100 mL of THF. The reaction was allowed to stir overnight. After the THF was removed by rotary evaporation, the mixture was extracted with CH_2Cl_2 , and the organic extract was dried over MgSO_4 . A ^1H NMR spectrum was recorded to check if the reaction was completed, and if not, the same procedure was repeated. The reaction mixture was concentrated in vacuo to give the desired product: yield 32%; ^1H NMR (300 MHz, CDCl_3) δ 2.50 (m, 2H, CH_2CH_2), 2.95 (m, 2H, CH_2CH_2), 7.37 (m, 6H, HC=C and Ar), 8.42 (s, 1H, HC=C), 11.21 (s, 1H, OH); ^{13}C { ^1H } NMR (75 MHz) δ 22.76, 27.16, 115.29, 128.60, 128.72, 129.77, 129.77, 129.86, 135.15, 176.54, 185.76; HRMS m/z calcd for $\text{C}_{13}\text{H}_{13}\text{O}_2$ 201.0916, obsd 201.0920.

2-[(3,4-Dimethoxyphenyl)methyl]amino-7-benzylidene-5,6-dihydro-5H-1-pyridine-3-carboxylic Acid, Ethyl Ester (12). A flame-dried 500-mL round-bottom flask was charged with 9.55 g (34 mmol) of **9** in 250 mL of dry THF. To this was added 9.55 g (34 mmol) of **10**, and the mixture was allowed to stir for 8 h under N_2 . The solvent was then removed by rotary evaporation, resulting in an orange residue. The product was purified by silica gel chromatography (hexanes/EtOAc = 2:1): yield 8.14 g (53.9%); mp 128–133 °C; ^1H NMR (300 MHz, CDCl_3) δ 1.37 (t, 3H, CH_2CH_3), 2.94 (m, 2H, CH_2CH_2), 3.11 (m, 2H, CH_2CH_2), 3.86 (s, 6H, OCH_3), 4.30 (q, 2H, CH_2CH_3), 4.80 (d, 2H, CH_2Ar), 7.19 (m, 9H, Ar and HC=C), 8.05 (s, 1H), 8.34 (t, 1H, NH); ^{13}C { ^1H } NMR (75 MHz, CDCl_3) δ 14.34, 27.24, 29.12, 44.90, 55.86, 55.93, 60.54, 105.49, 111.23, 111.58, 120.14, 124.09, 126.36, 127.16, 128.49, 129.20, 132.89, 136.55, 137.58, 141.75, 148.03, 148.97, 158.44, 163.72, 167.64. Anal. Calcd for $\text{C}_{27}\text{H}_{28}\text{N}_2\text{O}_4$: C, 72.95; H, 6.35. Found: C, 72.88; H, 6.39.

2-[(3,4-Dimethoxyphenyl)methyl]amino-5,6-dihydro-7H-1-pyridine-7-one-3-acetic Acid, Ethyl Ester (14). **12** (4.2 g, 9 mmol) was dissolved in 50 mL of H_2O /150 mL of THF, and 4.32 mL of OsO_4 (2.5% solution in 2-methyl-2-propanol) was added. The mixture was stirred for 20 min, and 4.78 g (24.65 mmol) of NaIO_4 was then added in portions over 40 min. The mixture was allowed to stir for 24 h. THF was then removed under reduced pressure. Water was added to the residue, and it was extracted with CH_2Cl_2 . The combined CH_2Cl_2 layers were washed with sodium bisulfite. After the solution was dried with MgSO_4 , the CH_2Cl_2 was removed by rotary evaporation. The residue was purified by silica gel chromatography (hexanes/EtOAc = 3:1, then 2:1): yield 2.1 g (65.6%); mp 142–145 °C; ^1H NMR (300 MHz, CDCl_3) δ 1.39 (t, 3H, CH_2CH_3), 2.71 (t, 2H, CH_2CH_2), 2.97 (t, 2H, CH_2CH_2), 3.85 (s, 3H, OCH_3), 3.88 (s, 3H, OCH_3), 4.33 (q, 2H, CH_2CH_3), 4.71 (d, 2H, CH_2Ar), 6.92 (m, 3H, Ar), 8.32 (s, 1H), 8.361 (s, 1H, NH); ^{13}C { ^1H } NMR (75 MHz, CDCl_3) δ 14.2, 22.4, 35.6, 45.2, 55.9, 61.5, 111.2, 111.9, 120.2, 131.6, 137.1, 139.3, 148.2, 148.9, 155.8, 158.6, 166.7, 205.9. Anal. Calcd for $\text{C}_{20}\text{H}_{22}\text{N}_2\text{O}_5$: C, 64.65; H, 6.02. Found: C, 64.85; H, 5.99.

2-[(3,4-Dimethoxyphenyl)methyl]amino-7-pyrrolidinyl-1-pyridineacetic Acid, Ethyl Ester (16). A 250-mL round-bottom flask was charged with 2.23 g (6.21 mmol) of **14** in 100 mL of THF. To this was added 60 mg of toluenesulfonic acid followed by the addition of 2.6 g (18 mmol) of 1-(trimethylsilyl)pyrrolidine. The reaction was allowed to stir at room temperature for 23 h. The THF was removed under vacuum. This compound was checked by ^1H NMR and used for the next step without further purification: ^1H NMR (300 MHz) 1.31 (t, CH_2CH_3 , 3H), 1.84 (2H), 2.31 (s, 2H), 3.14 (s, 2H), 3.20 (t, 2H), 3.45 (t, 2H), 3.80 (s, $\text{Ph}(\text{CH}_3)_2$, 6H), 4.25 (q, CH_2CH_3 , 2H), 4.66 (d, CH_2Ar , 2H), 5.33 (s, HC=C, 1H), 7.22 (m, H), 8.01 (s, para pyridine proton, 1H), 8.49 (t, NH, 1H).

α -[2-[(3,4-Dimethoxyphenyl)methyl]amino]-5,6-dihydro-3-(ethoxycarbonyl)-7-oxo-5H-1-pyridin-6-yl]- α -[2-[(3,4-dimethoxyphenyl)methyl]amino]-3-(ethoxycarbonyl)-8-oxo-5,6,7,8-tetrahydroquinolin-7-yl]acetic Acid, Ethyl Ester (18). A round-bottom flask was charged with 0.29 g (0.62 mmol) of **16** in 25 mL of dry THF, and 0.24 g (0.52 mol) of **17** in 10 mL of THF was added. This reaction was allowed to stir at 40 °C for 12 h, and then 0.01 N HCl (4 mL) was added and the reaction stirred for another 8 h. The mixture was neutralized by adding saturated NaHCO_3 and then extracted with CH_2Cl_2 . The organic layer was dried over Na_2SO_4 , and solvent was removed by rotary evaporation. The product was obtained after chromatography as a mixture of stereoisomers (EtOAc/hexanes = 1:3): MS-Cl (MH^+ = 839); ^1H NMR (300 MHz, CDCl_3) δ 1.14 (m, 9H, CH_2CH_3), 2.88 (m, 9H, $\text{CH}_2\text{CHCHCHCH}_2\text{CH}_2$), 3.72 (m, 12H, OCH_3), 4.02 (m, 6H, CH_2CH_3), 4.59 (m, 4H, CH_2Ar), 6.9 (m, 8H, Ar), 8.05 (m, 4H, NH); ^{13}C { ^1H } NMR (75 MHz, CDCl_3) δ 14.14 (m), 28.04

(m), 45.97 (m), 50.85 (m), 55.81, 61.04 (m), 111.06 (m), 120.17 (m), 126.88 (m), 131.65 (m), 135.31 (m), 138.79 (m), 141.78, 148.0, 148.83 (m), 1555.3 (m), 156.53, 158.50, 166.43 (m), 171.41 (m), 196.13 (m), 204.97 (m); HRMS m/z calcd for $C_{45}H_{51}N_4O_{12}$ 839.3503, obsd 839.352.

2,11-Bis[(3,4-dimethoxyphenyl)methyl]amino]-6,8-dihydro-5H-pyrido[3',2':5,6]cyclohexa[1,2-b]pyrido[2',3':4]cyclopenta[1,2-e]pyridine-3,7,10-tricarboxylic Acid, Triethyl Ester (19). A 5-mL round-bottom flask was charged with 290 mg of **18** and 2 mL of glacial acetic acid. To this mixture was added 80 mg of dry NH_4OAc . The reaction was allowed to stir at 110 °C for 3 h. The reaction mixture was neutralized with saturated $NaHCO_3$ and then extracted with CH_2Cl_2 . The product was purified by silica gel chromatography and crystallized from EtOAc and CH_2Cl_2 : yield 28%; mp 194–196 °C; 1H NMR (300 MHz, $CDCl_3$) δ 1.58 (m, 9H, CH_2CH_3), 2.81 (t, 2H, CH_2CH_2), 3.19 (t, 2H, CH_2CH_2), 3.63 (s, 2H, CH_2), 3.75 (m, 12H, OCH_3), 4.27 (m, 4H, CH_2CH_3), 4.46 (q, 2H, CH_2CH_3), 4.79 (d, 2H, CH_2Ar), 4.87 (d, 2H, CH_2Ar), 6.9 (m, 6H, Ar), 7.99 (s, 1H, para pyridine proton), 8.16 (t, 1H, NH), 8.30 (s, 1H, para pyridine proton), 8.37 (t, 1H, NH); ^{13}C $\{^1H\}$ NMR (75 MHz, $CDCl_3$) δ 14.33, 25.98, 32.03, 45.06, 45.19, 55.71, 55.79, 60.75, 60.83, 61.86, 105.84, 106.47, 111.02, 111.13, 111.77, 112.38, 120.42, 120.67, 120.97, 124.68, 132.17, 132.81, 133.70, 135.50, 136.47, 138.96, 139.44, 147.87, 148.75, 148.89, 152.82, 153.99, 157.88, 159.10, 161.29, 166.28, 167.28, 167.55; HRMS m/z calcd for $C_{45}H_{47}N_5O_{10}$ 817.3322, obsd 817.3333.

2,11-Diamino-6,8-dihydro-5H-pyrido[3',2':5,6]cyclohexa[1,2-b]pyrido[2',3':4]cyclopenta[1,2-e]pyridine-3,7,10-tricarboxylic Acid, Triethyl Ester (Free Base 2). Compound **19** (60 mg) was dissolved in 1 mL of THF under N_2 , and 32 μ L of anisole was added, following by 40 μ L of H_2SO_4 (36 N). The mixture was stirred for 21 h and then neutralized with 2.5 N NaOH. The crude product was purified by silica gel chromatography (EtOAc/MeOH = 9:1) and further purified by recrystallization from EtOAc: yield 70%; mp 220 °C dec; 1H NMR (300 MHz, $CDCl_3$) δ 1.39 (m, 9H, CH_2CH_3), 2.8 (t, 2H, CH_2CH_2), 3.185 (t, 2H, CH_2CH_2), 3.838 (s, 2H, CH_2), 4.29 (q, 4H, CH_2CH_3), 4.425 (q, 2H, CH_2CH_3), 6.57 (br, 4H, NH_2), 7.92 (s, 1H), 8.18 (s, 1H); ^{13}C $\{^1H\}$ NMR (75 MHz, $CDCl_3$) δ 14.27, 25.51, 25.60, 32.27, 60.78, 61.80, 105.79, 106.55, 121.96, 126.01, 133.84, 135.20, 136.30, 139.11, 139.30,

151.59, 153.53, 156.77, 158.65, 159.91, 160.68, 165.80, 166.67, 166.91. HRMS m/z calcd for $C_{27}H_{27}N_5O_6$ 517.1961, obsd 517.1970.

2,11-Diamino-6,8-dihydro-5H-pyrido[3',2':5,6]cyclohexa[1,2-b]pyrido[2',3':4]cyclopenta[1,2-e]pyridine-3,7,10-tricarboxylic Acid, Triethyl Ester, Monoprotonated Tetrakis(3,5-bis(trifluoromethyl)phenyl)borate Salt (2). Free base **2** (20 mg, 0.04 mmol) was dissolved in a minimum amount of CH_2Cl_2 , and then 0.95 equiv of picric acid was added to the solution. Picrate **2** was obtained by crystallizing from CH_2Cl_2 and EtOAc. Picrate **2** was then mixed with 1 equiv of sodium tetrakis(3,5-bis(trifluoromethyl)phenyl)borate in $CHCl_3$. The mixture was allowed to stir for 2 days and then filtered through Celite. The solvent was removed, and the resulting residue was dried over P_2O_5 : yield 31.5 mg, 59%; mp 80–82 °C; 1H NMR (300 MHz) δ 1.39 (m, 9H, CH_2CH_3), 2.99 (t, 2H, CH_2CH_2), 3.47 (t, 2H, CH_2CH_2), 4.10 (s, 2H, CH_2), 4.35 (q, 4H, CH_2CH_3), 4.495 (q, 2H, CH_2CH_3), 6.91 (b, 4H, NH_2), 7.46 (s, 4H), 7.66 (s, 8H), 8.50 (s, 1H), 8.53 (s, 1H); ^{13}C $\{^1H\}$ NMR (75 MHz) δ 13.82, 14.11, 23.45, 23.88, 33.36, 61.72, 62.88, 63.28, 108.77, 112.00, 117.40, 117.45, 119.09, 121.93, 122.70, 126.32, 123.20, 129.07, 129.92, 134.19, 136.88, 138.08, 142.95, 147.22, 161.33, 163.76, 164.14, 166.38. Anal. Calcd for $C_{59}H_{39}BF_4N_5O_6$: C, 51.29; H, 2.8. Found: C, 50.04; H, 2.8.

Acknowledgment. We gratefully acknowledge support of this work by the Searle Foundation (Chicago Community Trust) and an NSF-PYI award to E.V.A. We also thank Drs. Wayne Jones and Diane Kneeland for helpful discussions concerning fluorescence quenching.

Supplementary Material Available: Derivation of a form of the Benesi–Hildebrand equation showing that the concentration of the emitting species can be varied (1 page). This material is contained in many libraries on microfiche, immediately follows this article in the microfilm version of the journal, and can be ordered from the ACS; see any current masthead page for ordering information.